Research Article Open Access

Memduh Kurtulmuş*

Artificial Neural Network Modelling for Prediction of SNR Effected by Probe Properties on Ultrasonic Inspection of Austenitic Stainless Steel Weldments

https://doi.org/10.1515/chem-2018-0056
received January 24, 2018; accepted March 27, 2018.

Abstract: Many austenitic stainless steel components are used in the construction of nuclear power plants. These components are joined by different welding processes, and radiation damages occur in the welds during the service life of the plant. The plants are inspected periodically with ultrasonic test methods. Many ultrasonic inspection problems arise due to the weld metal microstructure of austenitic stainless steel weldments. The present research was conducted in order to describe the affects of probe angle and probe frequency of both transversal and longitudinal wave probes on detecting the defects of austenitic stainless steel weldments. Feed forward back propagation artificial neural network (ANN) models have been developed for predicting signal to noise ratio (SNR) of transversal and longitudinal wave probes. Input variables that affect SNR output in these models are welding angle, probe angle, probe frequency and sound path. Of the experimental data, 80% is used for a training dataset and 20% is used for a testing dataset with 10 neurons in hidden layers in developed ANN models. Mean absolute error (MAE) and mean absolute percentage error (MAPE) types are calculated as 0.0656 and 16.28%, respectively, to predict performance of ANN models in a transversal wave probe. In addition, MAE and MAPE are calculated as 0.0478 and 18.01%, respectively, for performance in a longitudinal wave probe.

Keywords: Austenitic stainless steel welding; Ultrasonic testing; Signal-to-noise ratio; Artificial Neural Networks
PACS – 07.05.Mh, 06.60.Vz, 81.20.Vj.

1 Introduction

Austenitic steels are non-magnetic stainless steels that contain high levels of chromium and nickel and low levels of carbon. Known for high resistance to corrosion, high strength, high creep properties and excellent formability, austenitic steels are the most widely used grade of stainless steel [1]. Austenitic stainless steels are used extensively at nuclear power plants as the main material of construction for process vessels and pipework. Stainless steel assemblies are visible throughout any particular plant. Austenitic stainless steel parts are joined by various welding processes. The atoms of austenitic steels have a face centered cubic structure at all temperatures. Therefore, the macrocrystalline structure of an austenitic weld is established when it solidifies and the austenitic phase forms long columnar dendritic grains, which grow along the directions of maximum heat loss during cooling. These coarse dendritic grains have extreme anisotropic properties [2].

Ultrasonic testing is the dominant non-destructive testing process utilized to detect under surface defects in nuclear power plants [3]. The heterogeneous and anisotropic structures exhibited by austenitic steel multi-pass welds cause difficulties in the interpretation of ultrasonic testing results [4]. One of the most serious problems in the inspection of austenitic welds is the presence of large spurious signals, which have been attributed to the characteristic acoustic impedance mismatch existing between the metals that make up the weld [4]. The characteristic large, mostly orientated and dendritic weld grains lower the ultrasonic sound velocity and distribute the sound in multiple directions, causing the sound beam to twist. [5]. The grain boundaries, the weld root and the weld fusion line also cause scattering of the sound [6]. These factors lead a poor signal to noise ratio and a low defect detection ability [7]. Several attempts have been made to resolve this inspection problem. New probes have been produced [8] and some improvements have been achieved in ultrasonic testing methods [9-12]

***Corresponding author: Memduh Kurtulmuş,** Marmara University, Applied Science High School, Istanbul, Turkey, E-mail: memduhk@marmara.edu.tr

permitting higher signal to noise ratios and higher defect detection abilities in the inspection of austenitic stainless steel welds.

The intention of this study was to reveal the effects of probe properties on ultrasonic testing of austenitic weldments. The influences of probe type, sound length and probe frequency were investigated. From the test results, we developed feed forward back propagation artificial neural network (ANN) models for the prediction of signal to noise ratio (SNR) of transversal and longitudinal wave probes.

2 Materıals And Methods

A 20 mm thick SAE 304L austenitic stainless steel plate was used as the test case. The chemical properties of the plate are presented in Table 1. Four 250x150 mm welding test pieces were obtained from the plate by the laser cutting process. In the cutting operation the longitudinal direction of the piece was chosen cautiously in order to make the welding application parallel to the rolling direction of the plate. Standard 45° and 60° single-V weld groove workpieces [13] were obtained at a milling machine. The plates were welded by the shielded metal arc process (SMAW). ASP 308L electrodes were used in welding. Welding operations were done in the flat position without preheating. During welding each pass of the weld was controlled by the liquid penetrant test. The aim of this examination was to reveal any crack that might have occurred in the weld. At the end of the process, defect-free full penetration butt welds were obtained. After finishing the welding operation 1mm diameter and 20 mm deep holes were drilled in the middle of the weld metal.

The welds were inspected by the ultrasonic method using a KRAUTKRAMER USM 25S detector, which is a digital/analog pulse echo flaw detector. Prior to the inspection, the workpiece surface was lightly greased. The probes used in the experiment and their properties are shown in Table 2. In the tests the reference display was chosen as 40%. The signal to noise (S/N) ratio was calculated for each test. The measured S/N ratio gives the defect detection ability of a probe [14]. A high S/N ratio shows a high detect ability. In each test the sound path length was displayed directly on the screen of the detector. The butt joint, the drilled hole and position numbers of the ultrasonic test probes are schematically shown in Figure 1. The numbers indicate the probe described in Table 2.

Ethical approval: The conducted research is not related to either human or animals use.

Table 1: Chemical composition (% of mass) of the SAE 304L test plate.

C	Si	Mn	Cr	Ni	S	P
0,03	0,65	1,33	19,15	10,76	0,01	0,03

Table 2: The properties of the ultrasonic test probes.

Probe Position	Mode	Frequency (MHz)	Probe Angle
1	Tranversal	2	45
2	Tranversal	2	70
3	Tranversal	4	45
4	Tranversal	4	70
5	Longitudinal	1,8	45
6	Longitudinal	1,8	70
7	Longitudinal	4	45
8	Longitudinal	4	70

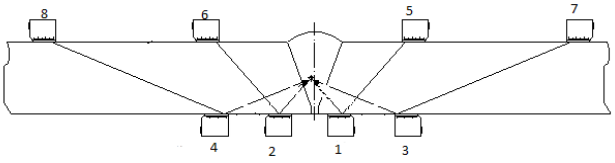

Figure 1: The probe positions in the tests.

3 Results And Discussıon

The results of the ultrasonic tests using the transversal probes are shown in Table 3. The test results illustrate that S/N ratio decreases with the increase in sound path length. The scattering increases with the length of the sound path, a factor that lowers the S/N ratio [1]. The 4MHz probes at similar sound path lengths gave higher S/N ratios than the 2MHz probes. The results of ultrasonic tests using the longitudinal probes are shown in Table 4. These test results illustrate that the S/N ratio decreases with the increase in sound path length. These results are in good agreement with the transversal probe results. The 1.8MHz probes at similar sound path lengths gave higher S/N ratios than the 4MHz probes. These results are contrary to the transversal probe results. Transversal 4MHz probes showed better defect detection than longitudinal 4MHz probes. Similar results were obtained in ultrasonic testing of austenitic stainless steel welds [4, 14].

Table 3: Results of Ultrasonic Tests using Transversal Probes.

Groove Angle	Probe Position	Probe Angle	4.0 MHz Frequency Probe		2.0 MHz Frequency Probe	
			Sound Path	S/N Ratio	Sound Path	S/N Ratio
45°	1	45°	15.08	16.5	14.63	13.0
45°	2	45°	15.90	16.0	15.42	12.5
60°	1	45°	17.36	15.5	16.94	12.0
60°	2	45°	18.02	15.0	17.33	11.5
45°	3	70°	25.77	15.0	23.09	11.0
45°	4	70°	26.46	14.0	23.85	11.5
60°	3	70°	28.91	14.5	28.97	10.5
60°	4	70°	29.21	13.0	29.64	10.5
45°	5	45°	41.67	11.5	42.07	9.5
45°	6	45°	43.74	12.5	43.56	9.0
60°	5	45°	44.80	11.0	44.97	8.5
60°	6	45°	46.96	10.0	45.73	9.0
45°	7	70°	81.75	9.0	82.98	7.5
45°	8	70°	81.96	9.5	83.18	8.0
60°	7	70°	83.70	9.5	86.39	7.0
60°	8	70°	84.28	8.5	88.61	6.5

Table 4: Results of Ultrasonic Tests using Transversal Longitudinal Probes.

Groove Angle	Probe Position	Probe Angle	4.0 MHz Frequency Probe		1.8 MHz Frequency Probe	
			Sound Path	S/N Ratio	Sound Path	S/N Ratio
45°	1	45°	15.25	15,0	13,64	12.5
45°	2	45°	15.40	15.5	13.77	12.0
60°	1	45°	15.82	15.0	15.41	16.5
60°	2	45°	16.08	14.0	15.91	16.0
45°	3	70°	26.18	12.0	29.93	12.5
45°	4	70°	26.43	10.5	30.08	13.5
60°	3	70°	26.95	11.5	34.73	12.5
60°	4	70°	27.38	11.5	36.38	12.5
45°	5	45°	43.14	8.0	42.38	12.5
45°	6	45°	44.08	7.5	43.10	12.0
60°	5	45°	45.72	6.5	45.03	11.5
60°	6	45°	46.14	7.0	45.88	12.0
45°	7	70°	86.83	3.5	87.75	10.5
45°	8	70°	87.44	5.0	88.40	10.0
60°	7	70°	88.17	4.0	91.20	10.5
60°	8	70°	89.22	4.0	92.34	9.5

Table 5.: Test probes and sound path length of tests.

Layer	Probe Characteristics	Transversal		Longitudinal	
Inputs	Probe Angle	45	60	45	60
	Probe frequency (MHz)	2	4	1,8	4
	Sound Path (mm)	15,08 – 86,61		13.64-92.34	
Outputs	SNR (dB)	6.5-16.5		3.5-16.5	

4 Developed Artificial Neural Network Models

ANN models have many applications in the optimization of welding parameters and analysis of quality control specifications [16, 17]. In this study, two ANN models were developed for both transversal and longitudinal probes, These models included four input variables: Welding Angle, Probe Angle, Probe Frequency and Sound Path. Feed forward back propagation ANN models have been used to predict the SNR. Since SNR depends on transversal and longitudinal wave probes, variables were changed parametrically according to data presented in Table 5.

Two ANN models for transversal and longitudinal wave probes were developed to predict SNR values in this study, and their prediction performances were compared. Both ANN models included 10 neurons in hidden layers. Thirty-two rows of data were obtained from the experiments and 80% of this dataset (26 rows of data) was used for training data and 20% (six rows of data) is used for validation of developed models. The input-output data can be actual or normalized. It is clear that using normalize data lead to better results. Normalized training and testing datasets of laboratory experiments are calculated using Equation (1).

$$X = (Xi-Xmin) / (Xmax-Xmin) \quad (1)$$

X = Normalized data Xi = Actual data
Xmin = Minimum value of actual data Xmax = Maximum value of actual data

In this study, the feed forward back propagation ANN model was preferred. The reasons for using the feed forward back propagation ANN model for multi-layered ANNs are that it is a global approximator and that it was the best performing ANN model under current conditions. Levenberg Marquardt was used as a training algorithm in feed forward back propagation ANN models that were developed. The Gradient Descent with Momentum (GDM) learning algorithm was applied as the learning algorithm utilizing Matlab software. Variables were normalized

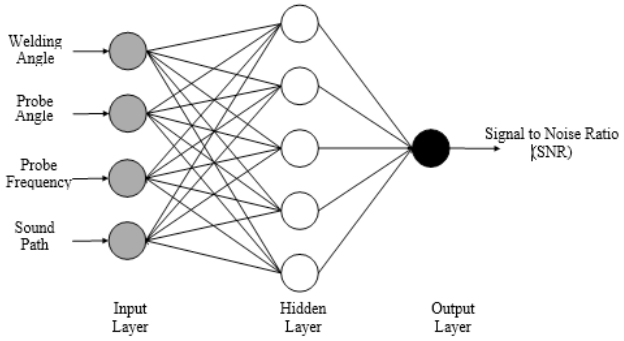

Figure 2: Structure of a developed ANN models.

Table 6: MAE and MAPE Values of 2 Developed ANN Models.

Wave probes	Transversal	Longitudinal
Ratio of training dataset	80%	80%
Ratio of testing dataset	20%	20%
Number of neurons in hidden layer	10	10
MAE	0.0656	0.0478
MAPE (%)	16.2855	18.0118

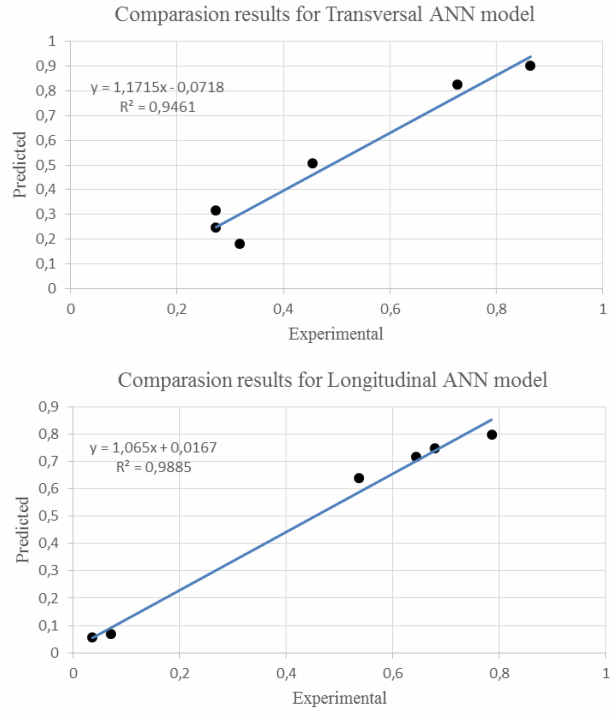

Figure 3: Regression Analysis Results of two Developed ANN Models.

between 0-1; therefore, the LOGSIG (Log-sigmoid) transfer function was preferred for the developed ANN models.

As a result of tests and analysis, the optimum topology of a network has been obtained with a specific number of epoch which is equal with 300. ANN models that have been developed consisted of four-neuron- input layers that represent inputs. The hidden layer is made of 10 neurons, and the output layer is made of one neuron. A structure which represents ANN's input, output and hidden layers are displayed in Figure 2. The ANN model thus developed has been run with the described properties.

As the last step of the study, two different ANN models are compared with the actual values after training processes have been completed. During the comparison, data MAE (Mean Absolute Error) and MAPE (Mean Absolute Percentage Error) were selected as the type of error with the help of Eq. (2) and Eq. (3) for validation of the ANN models. Resulting data are given in Table 6.

$$MAE = \frac{1}{n}\sum_{t=1}^{n} |At - Ft| \quad (2)$$

$$MAPE = \frac{100\%}{n}\sum_{t=1}^{n} \left|\frac{At-Ft}{At}\right| \quad (3)$$

where At is actual data, Ft is forecast at time t and n is the number of samples.

Comparisons between experimental and predicted values of the output variable of two developed ANN models are shown in Figure 3. MAE, MAPE and MSE (R2) values show that the prediction performances of these models were successful.

5 Conclusion

In this study, we found that an extended sound path decreased the detection of the discontinuities. In addition, the defect detection characteristics of transversal wave probes increased with the probe frequency, while the defect detection characteristics of longitudinal wave probes decreased with the probe frequency. Of the two probe types, the longitudinal wave probes were found to be superior in ultrasonic inspection tests of austenitic stainless steel weldment. Finally, a successful ANN model was developed.

Conflict of interest: Authors state no conflict of interest.

References

[1] Kurtulmus M., Buyukyildirim G., Yukler A.I., Optimum Ultrasonic Inspection Conditions of Butt Welded SAE 304L

Austenitic Stainless Steel, First South East European Welding Congress, Timisiora, Romania, 2006.
[2] Kemnitza P., Richtera U., Klüberb H., Nuc. Eng. Design, 1997, 174, 259-272.
[3] Moysan J., Apfel A., Comeloup G., Chassignole B., Int. J. Press. Vessels Piping, 2003, 80, 77- 85.
[4] Erhard A., Lucht B., Schulz E., Montag H. J., Wüstenberg H., Beine U., Non-Destr. Test. Journ., 2000, 5, 1-5.
[5] Chassignole B., Doudet L., Dupond O., Fouque T., Richard B., New Developments for the Ultrasonic Inspection of Austenitic Stainless Steel Welds, European Nuclear Conference, Versailles, France, 2005.
[6] Connolly G.D., Lowe M.J.S., Rokhlin S.I., Temple J.A.G., AIP Conf. Proc., 2008, 975, 1026- 1033.
[7] Anderson M.T., Cumblidge S.E., Steven R., Applying Ultrasonic Phased Array Technology to Examine Austenitic Coarse Grained Structures for Light Water Reactor Piping, 3rd EPRI Phased Array Inspection Seminar, Seattle, U.S.A., 2003.
[8] Kawanami S., Kurokawa M., Taniguchi M., Tada Y., Mitsubishi Heavy Industr. Tech. Review, 2001, 38, 121-125.
[9] Praveen A., Vijayarekha K., Abraham S.T., Venkatraman B., Ultrasonics, 2013, 53, 1288-1292.
[10] Moles M., Cancre F., AIP Conf. Proc., 2002, 615, 855.
[11] Schmerr L.W., Fundamentals of Ultrasonic Phased Arrays, Elsevier, London, U.K., 2015.
[12] Chardome V., Verhagen B., Non-Dest. Test. Cond. Monitor., 2008, 50, 490-492.
[13] AWS D1.1/2015 Structural Welding Code-Steel, AWS, 2015.
[14] Kurtulmus M., Fidaner O., Yukler A.I., Testing of Repair Welded Boiler Pipes of a Thermal Power Station, 13th International Energy Conference, Istanbul, Turkey, 2007.
[15] Kurtulmus M., Yukler A.I., Sci. Res. Essays, 2011, 6, 305-312.
[16] Ozcanli Y., Kosovali C., Beken M., ACTA Physica Polonica A, 2016, 130, 444.
[17] Tekin H.O., Manici T., Altunsoy E.E., Yilancioglu K., Yilmaz B., ACTA Physica Polonica A, 2017, 132, 967.